Diamond Anvil Measurement of Muon-Catalyzed Fusion Kinetics

The dμ/DT Collaboration

PSI BVR 55 Progress Report

February 7, 2023

Ara Knaian

Introduction

Fusion is an safe, abundant source of clean energy

Fusion of the deuterium in a stream of tap water could power a city.

Introduction

Plasma fusion requires stable 100,000,000 C plasma

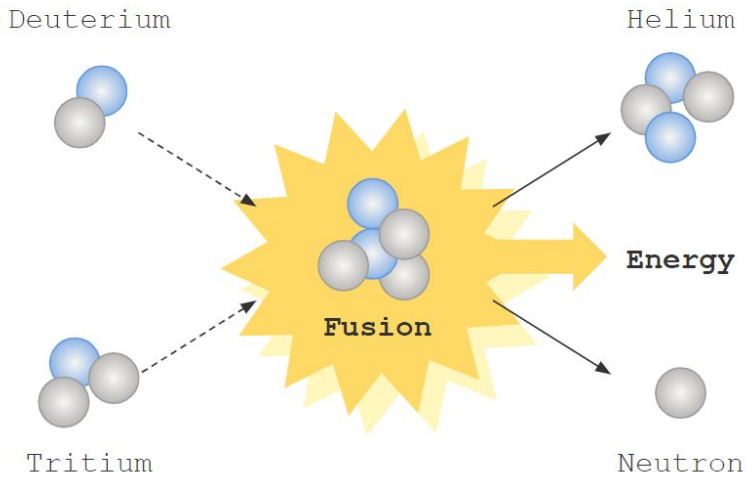

The deuterium-tritium fusion reaction has the highest cross section.

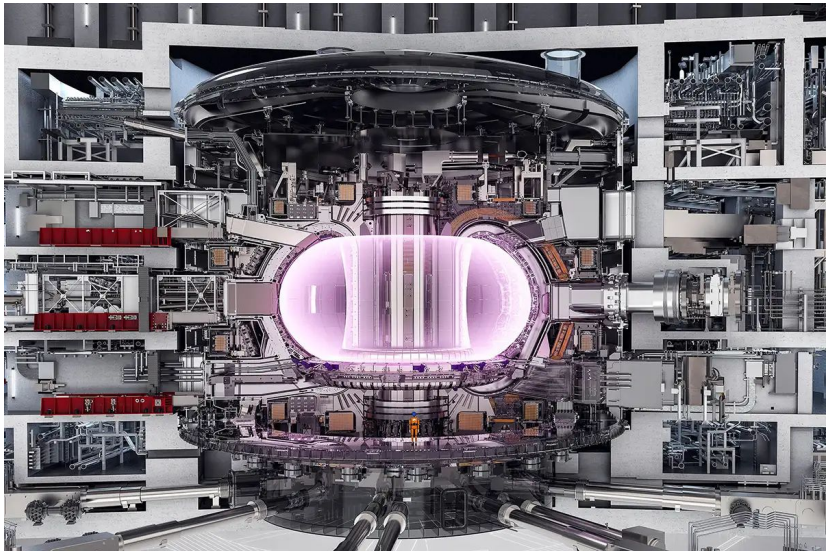

A cutaway view of the ITER tokamak, scheduled to burn DT in 2035.

Introduction

Muons can catalyze fusion reactions at lower temperature

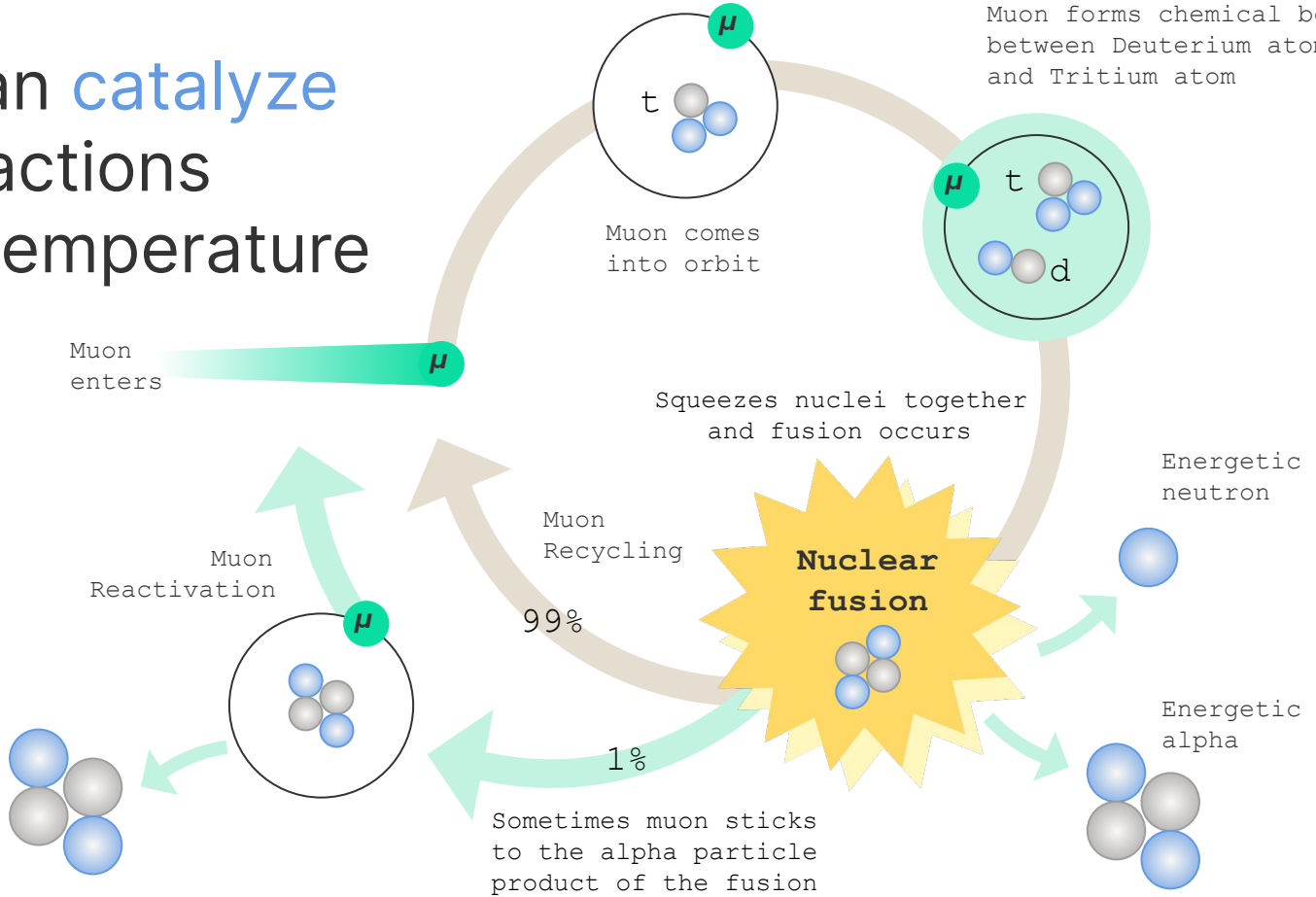

Cost of electricity versus physics parameters

Engineering breakeven

Target operating point for a reactor

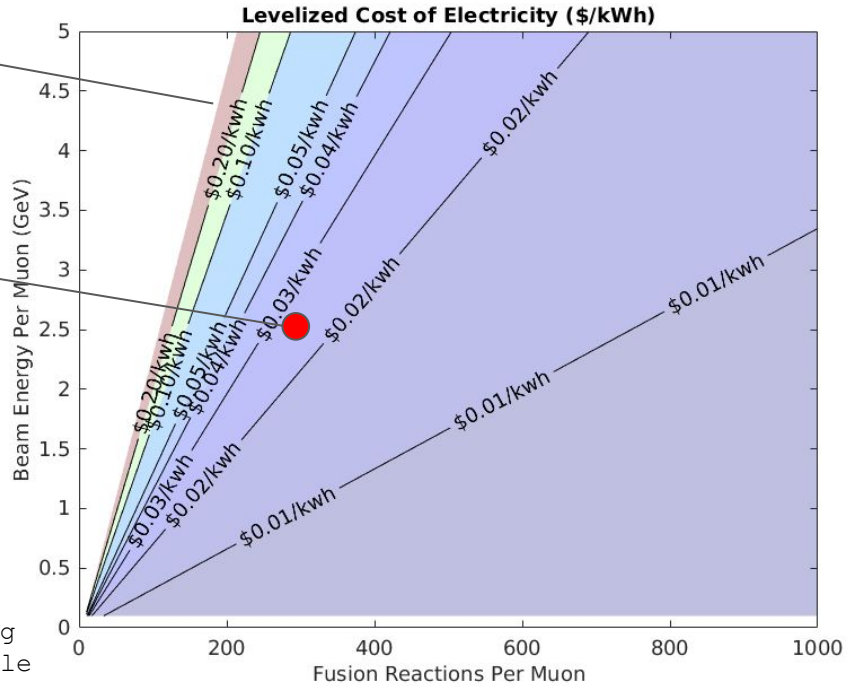

(Using a superconducting accelerator, Brayton cycle balance of plant, and revenge from heat sales.)

Cost of baseload power by source, $/kWh (1)

Coal	$0.089
Biomass	$0.077
Nuclear fission	$0.071
Gas:	$0.043

Target operating point:

Fusion (?): $0.025

(1) Levelized Costs of New Generation Resources in the Annual Energy Outlook 2023, US Energy Information Administration, Document #AEO2023

Fusion rate increases with temperature and density

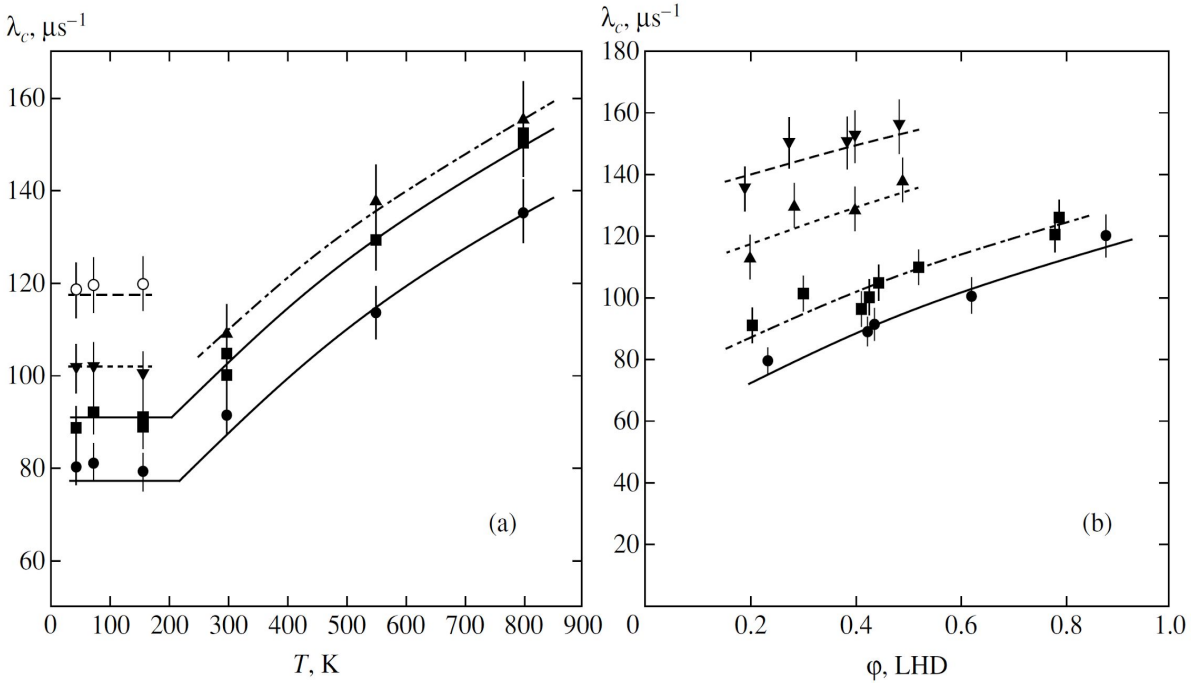

Experimental Data from JINR measurements on DT
Ref: V.R. Bom et. al, JETP, 2005

Sticking may decrease with density

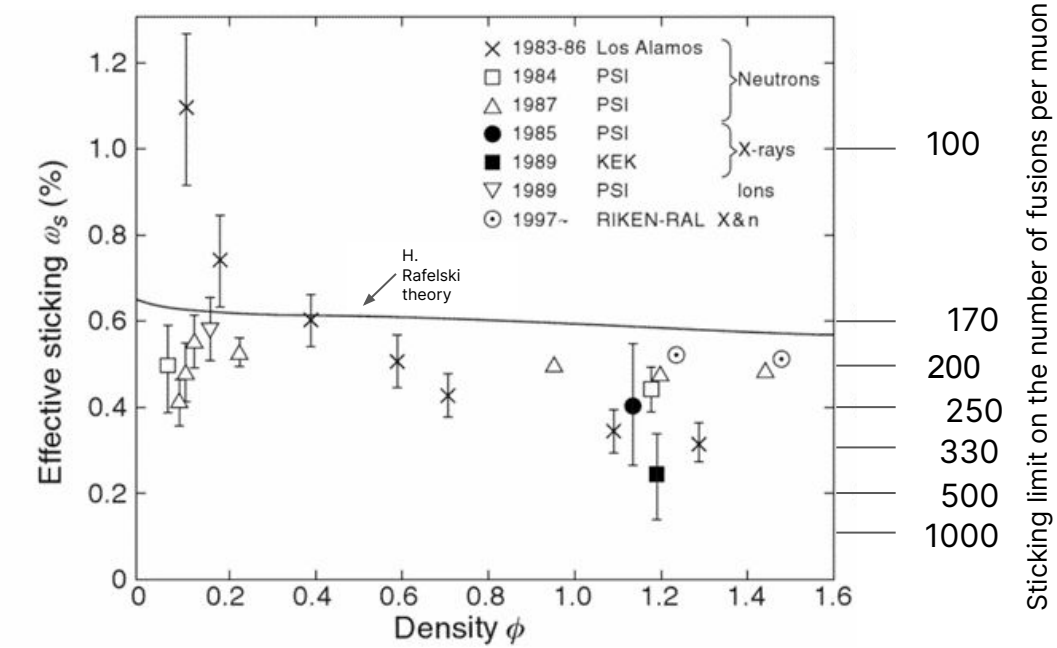

Ref: K. Nagamine, 2008

- Both experiment and theory predict that sticking decreases with density.
- Data from four experimental groups is shown.
- At high density, the measured sticking is uniformly lower (better) than predicted by theory
- Density is stated as a fraction of liquid hydrogen atomic number density.

Our Experiment

Goals of our collaboration

- Measure DT cycling rate and sticking fraction at high density and temperature
- Create open-source physics process models for GEANT4

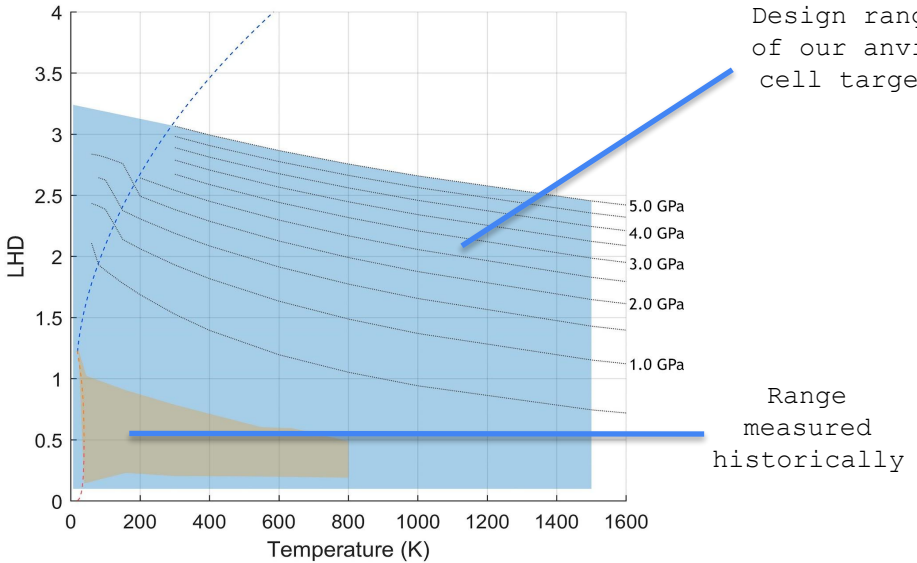

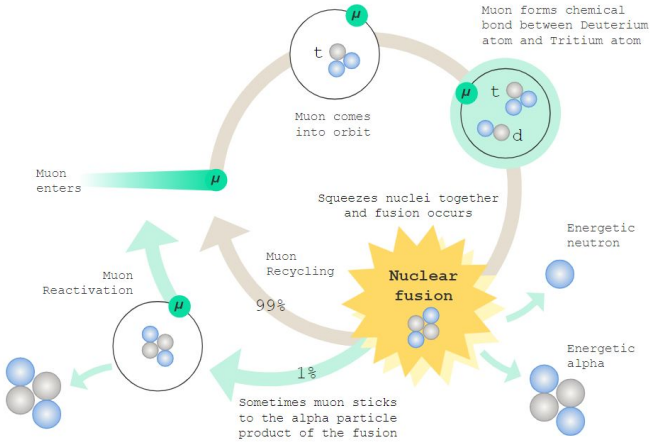

Our Experiment

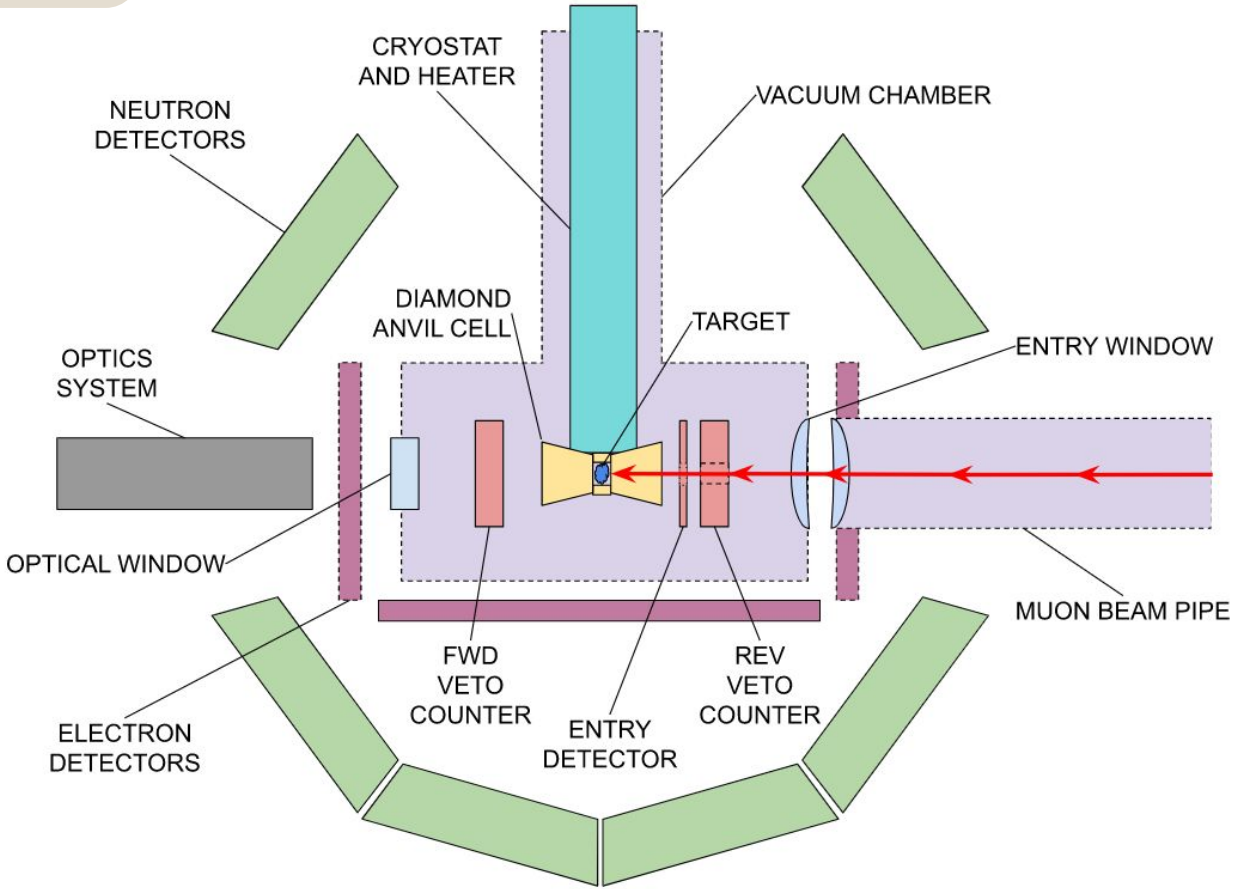

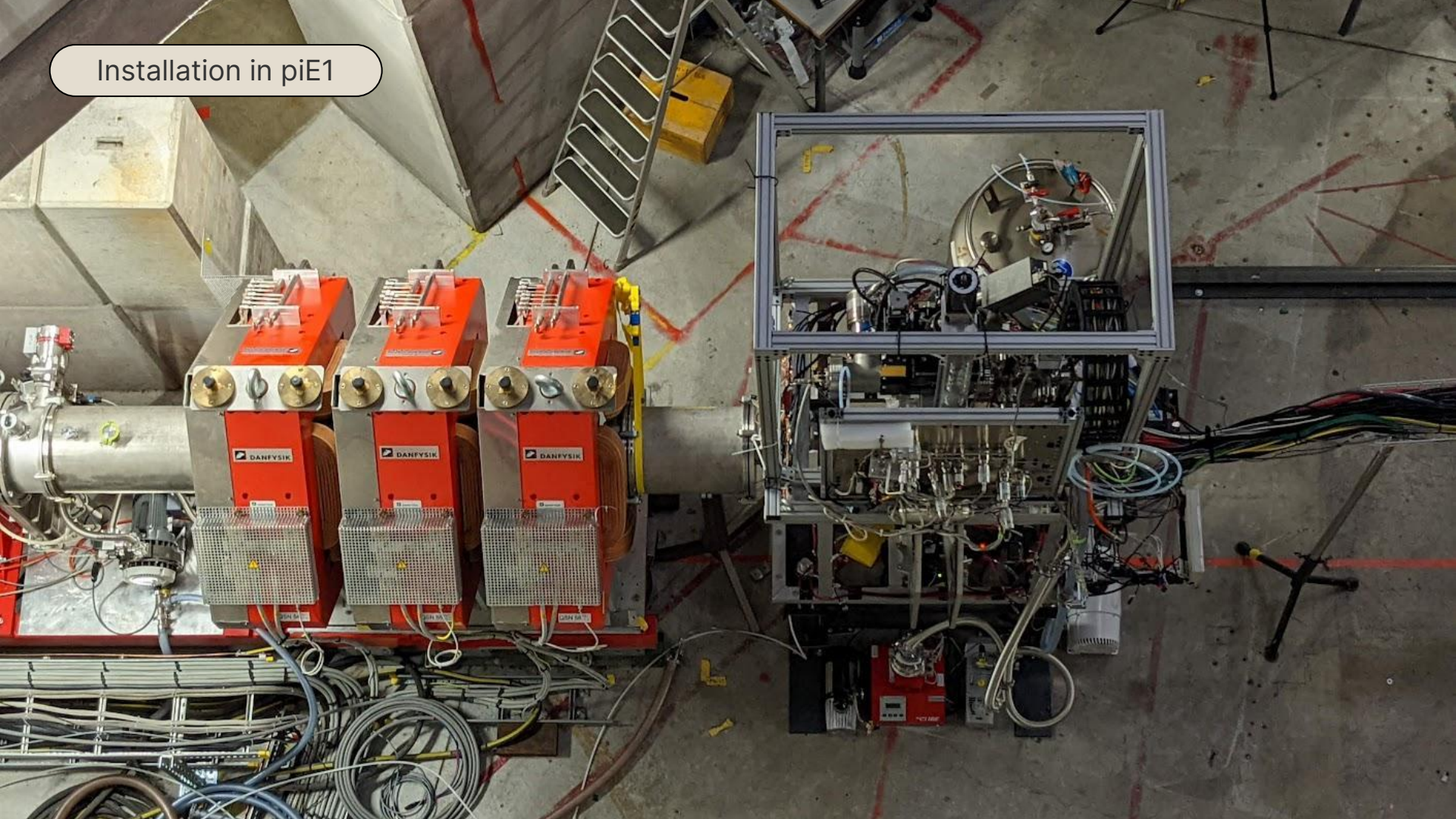
Installation in piE1
DANFYSIK
DANFYSIK
DANFYSIK

Section view of the target chamber

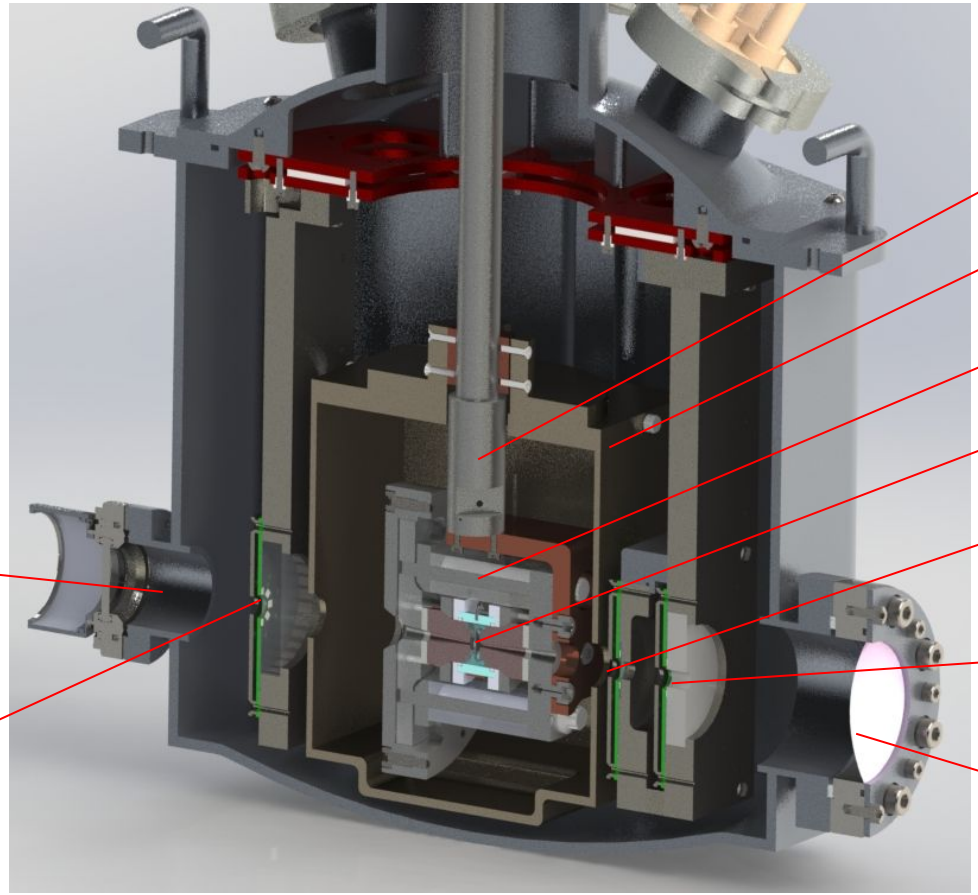

Neutron and electron detectors surround the target

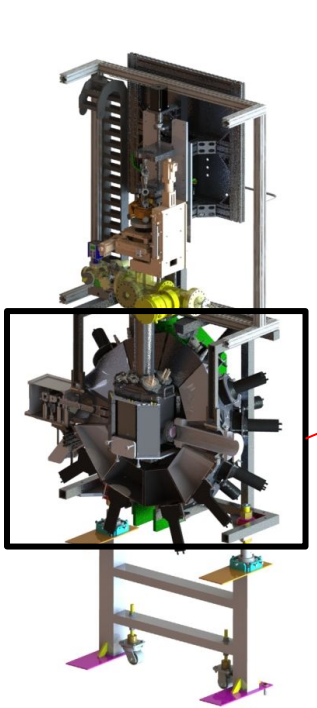

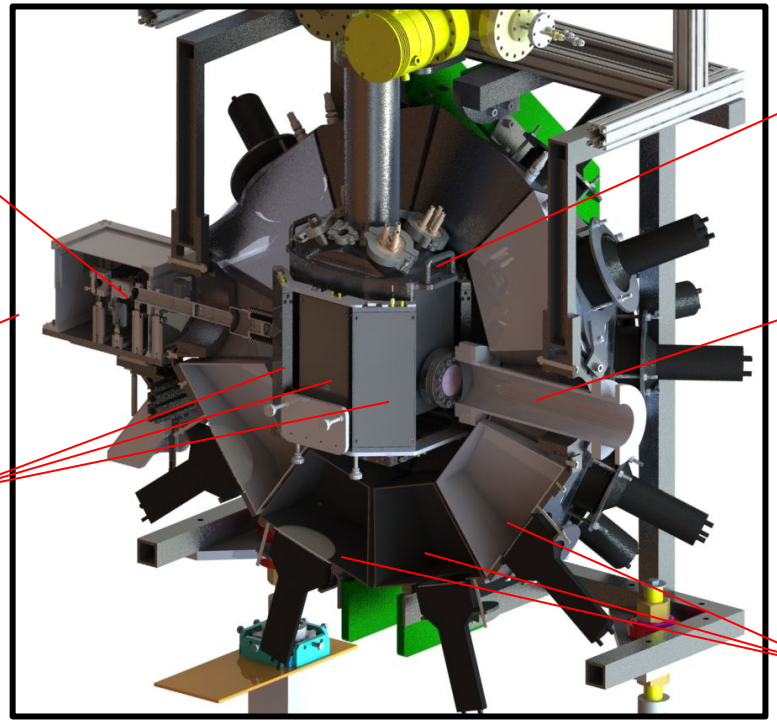

Optics System

Electron Detectors

Lower Vacuum Chamber (containing target)

Beam Line Extension

Neutron Detectors

Detector Performance

Neutron detector has 40-50% absolute efficiency

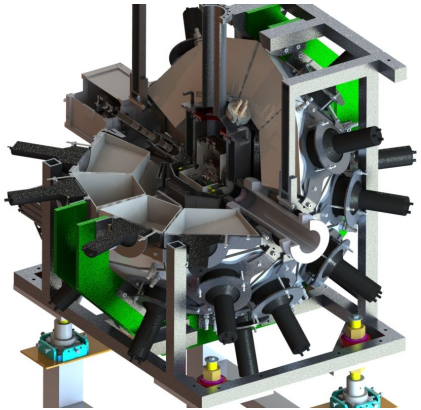

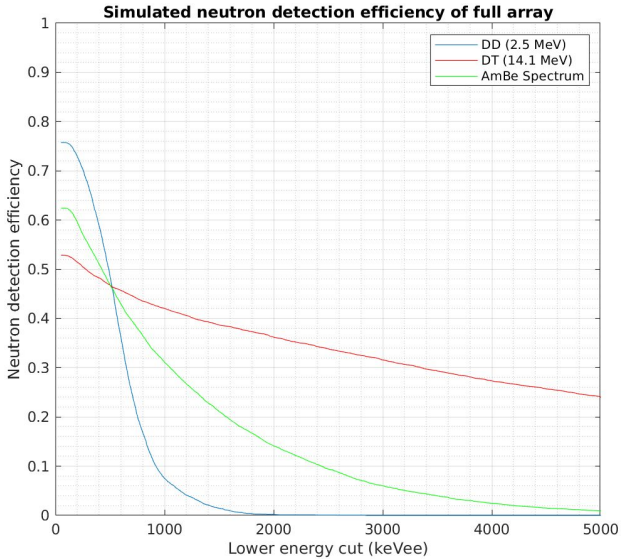

- 300 L of organic liquid scintillator
- Weighs about one ton
- ~ 87% solid angle
- Pulse shape discrimination allows identification of neutrons
- With DT, we will see events with order 100 neutron detections per muon

Measured spectra and rates align with simulation

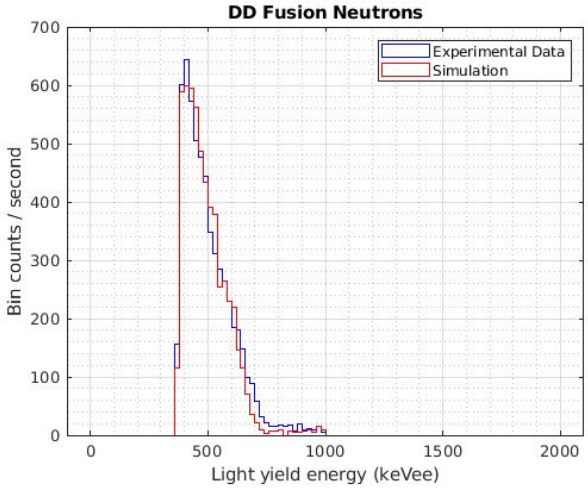

D-D Muon Catalyzed Fusion Neutrons

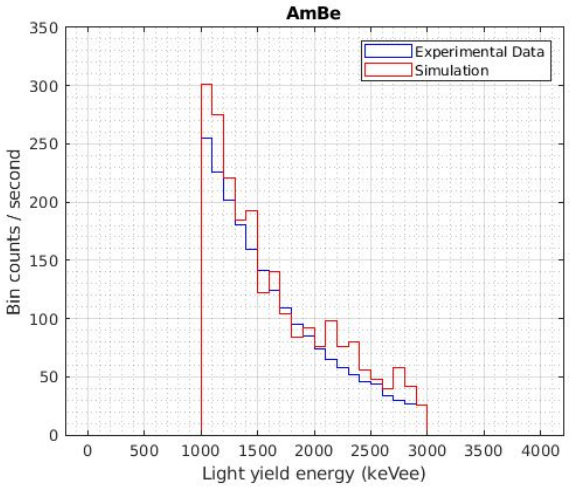

AmBe Neutron Source

+14%

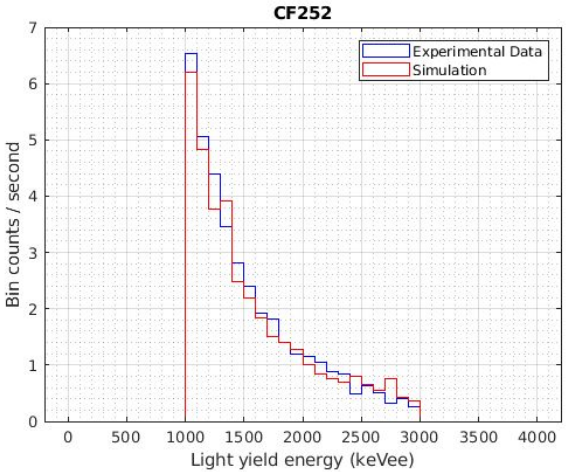

CF-252 Neutron Source

-9%


ED1
BEAM

Neutron detection between muon and electron

Liquid Hydrogen

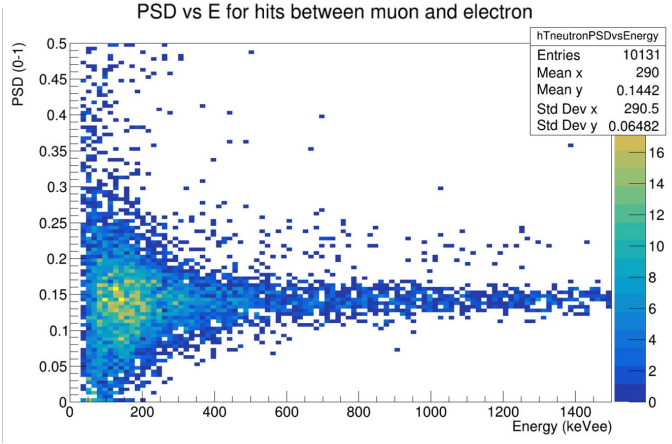

Liquid Deuterium

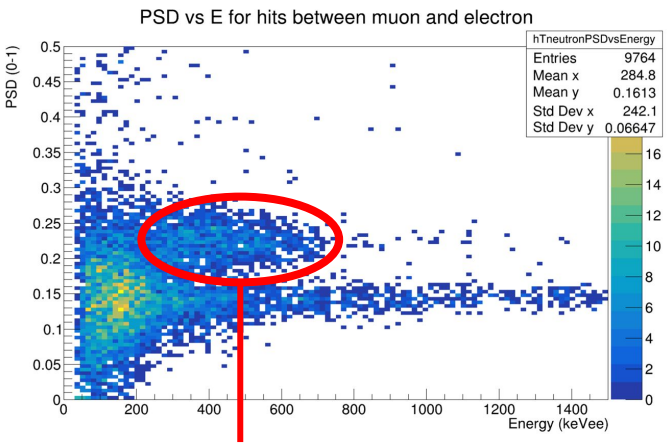

Fusion neutrons

Time Spectrum of Fusion Neutrons

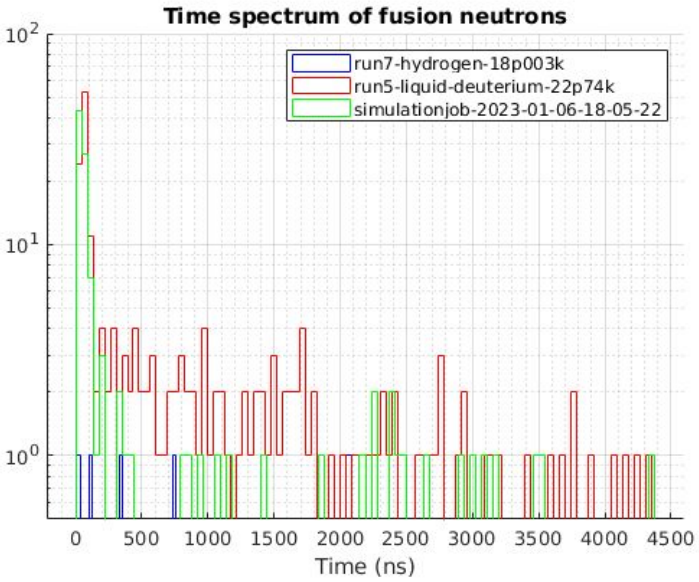

2022

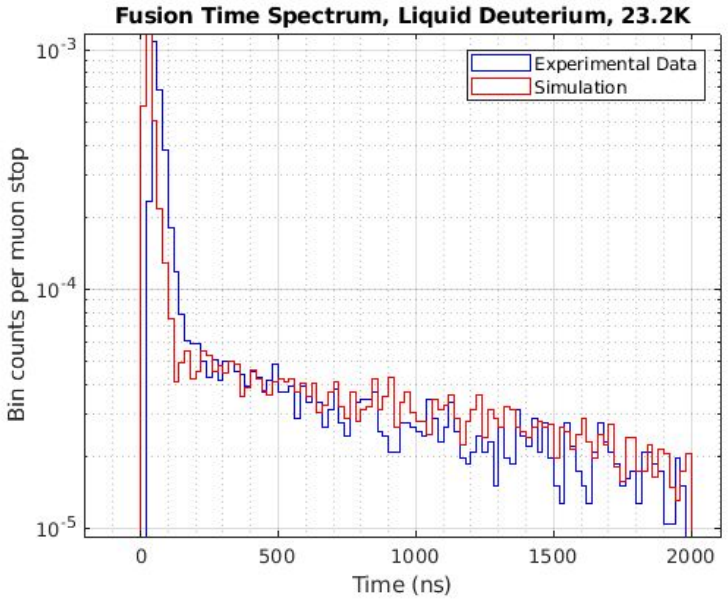

2023

Simulation reproduces measured backgrounds

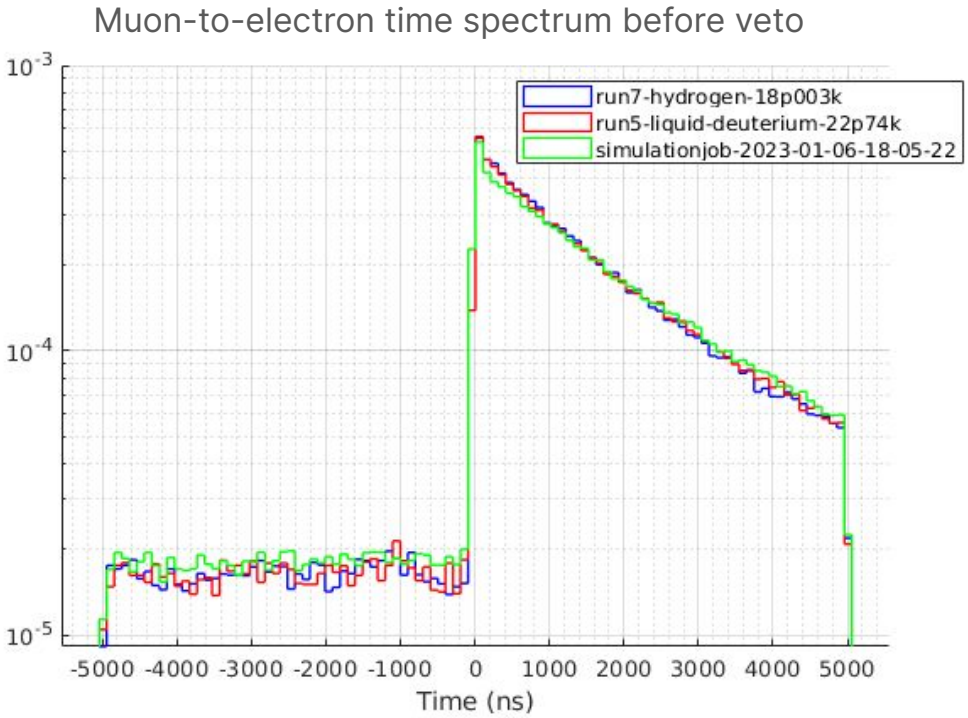

Compression of mineral oil to 4.5 GPa (2021)

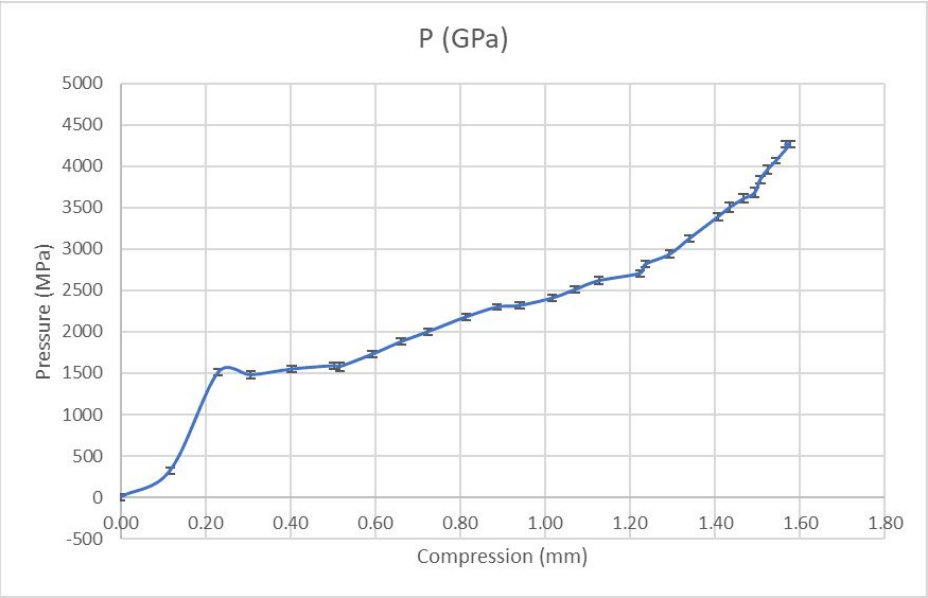

Merrill-Basset cell with Boehler-Almax cut diamonds installed in a breech configuration for large (cubic mm scale) sample volume.

Anvil cell in beam (2022)

Cryostat tip cools assembly to ~16 K, and provides heating to 800K

Pressurized helium membrane applies force to diamond, compressing target

Minichamber holding hydrogen gas for cooling

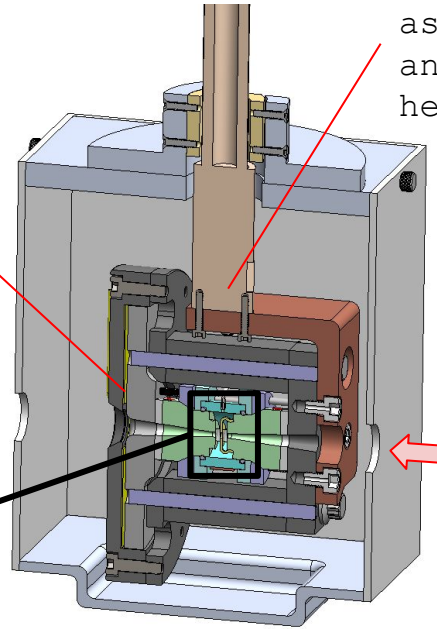

Beam entry

Aluminum gasket contains target

DAC seat carries force from He membrane to diamond

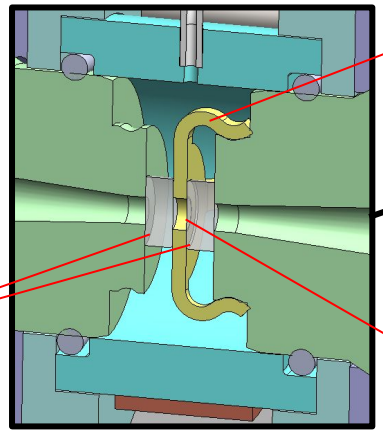

diamond anvils

Sample chamber is open during filling and cooling, then closed prior to pressurization

Anvil preparation at the MIT nanofabrication facility

Diamond anvils prepared for transport to PSI:

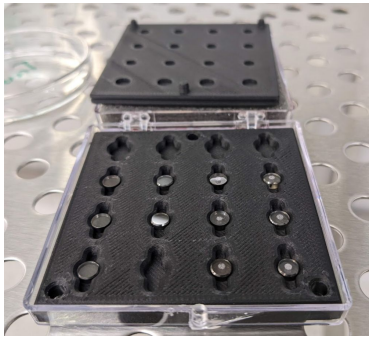

Drying diamond anvil after piranha clean & water rinse:

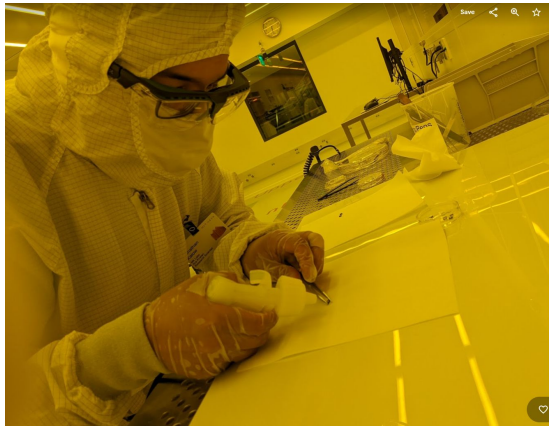

~1-30 μm ruby particles placed using mask:

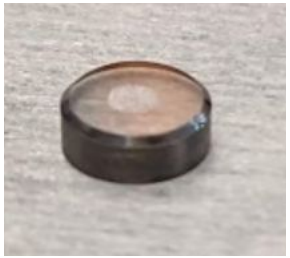

Diamond anvils loaded onto wafer in the atomic layer deposition reactor:

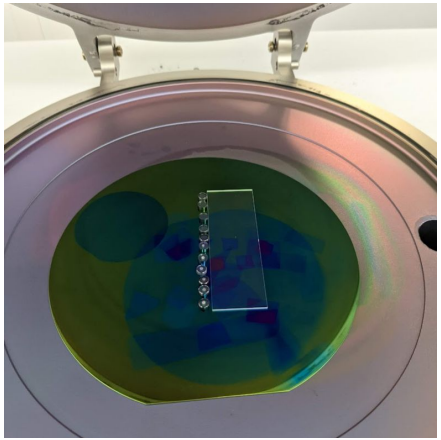

Diamond anvils fastened to seats using Stycast 1266, prior to cell assembly:

Optical Pressure Measurement

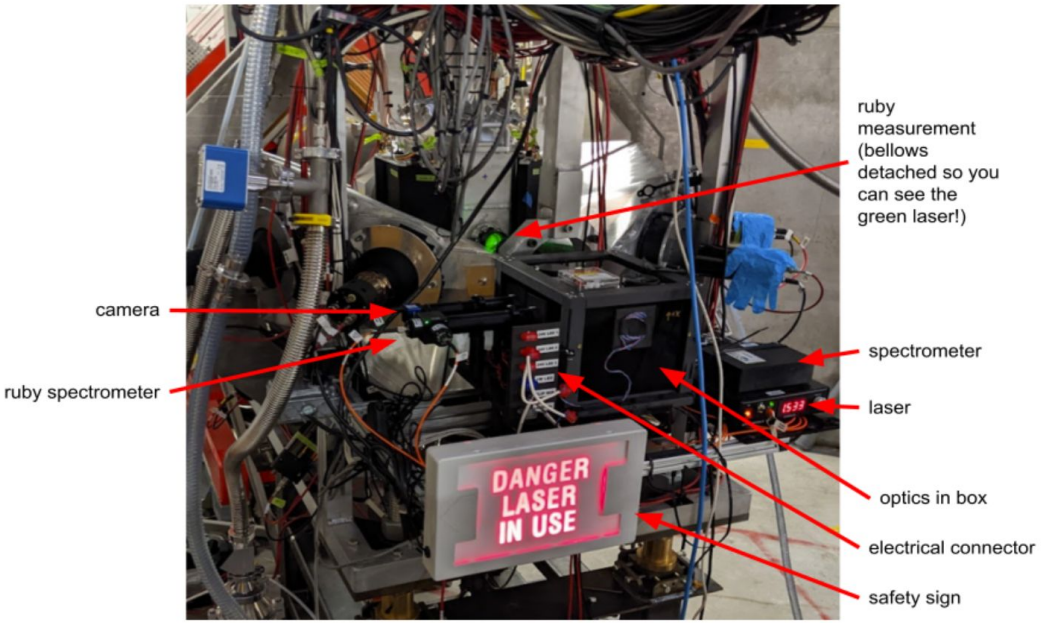

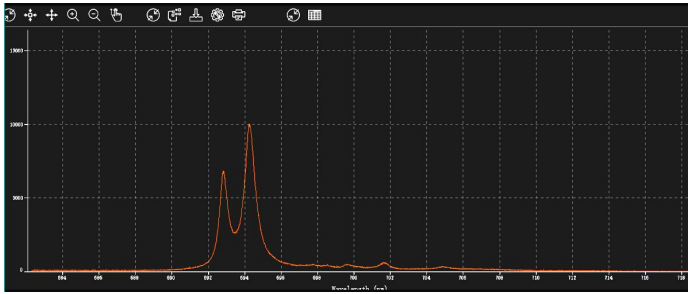

2022 Ruby Spectrum

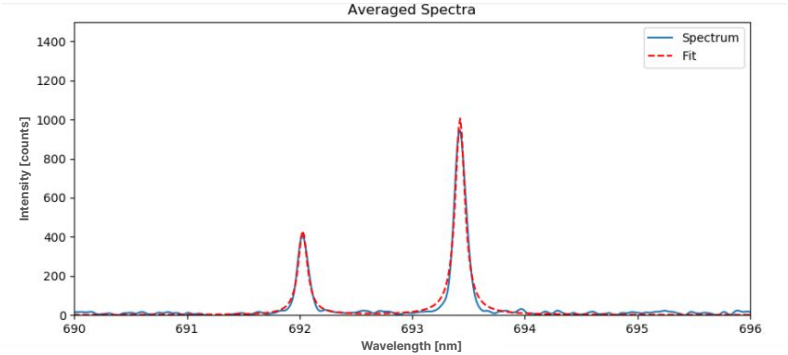

2023 Ruby Spectrum

In-system compression/heating of liquid argon (2023)

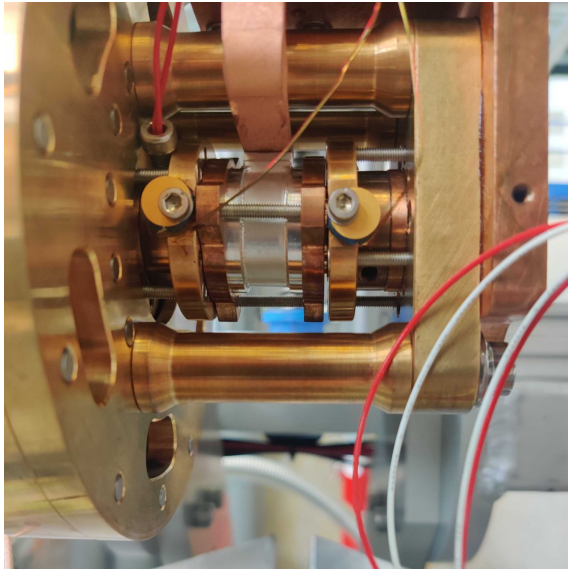

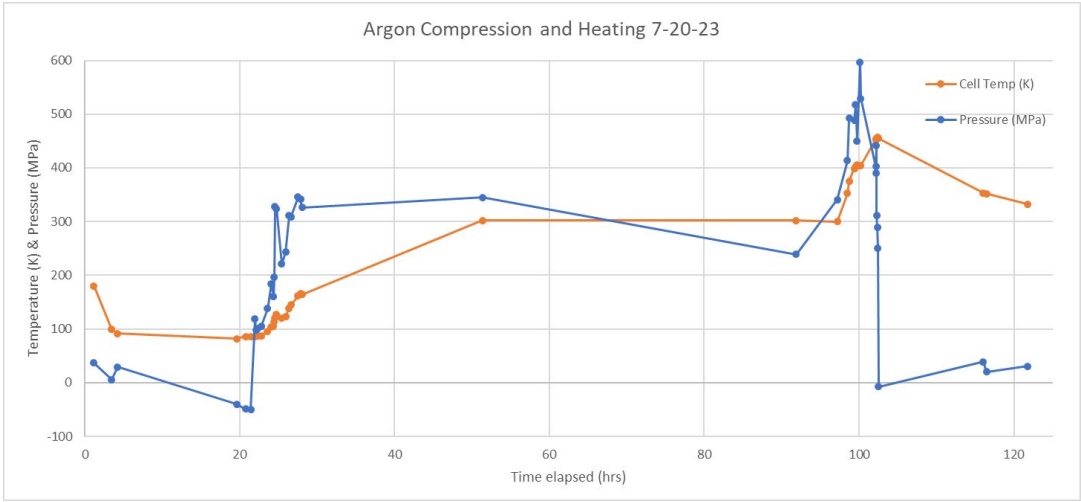

We used liquid nitrogen to cryogenically load liquid argon for testing. The sample wa compressed to 600 MPa and heated to 450 K. The sample was held under compression in vacuum for 80 hours.

In-system compression of **liquid hydrogen** (2024)

Key design changes:

- Beryllium copper body
- Replace spring-energized teflon seal with indium wire seal
- Replace sliding interface with bellows
- Use two gas membranes in series

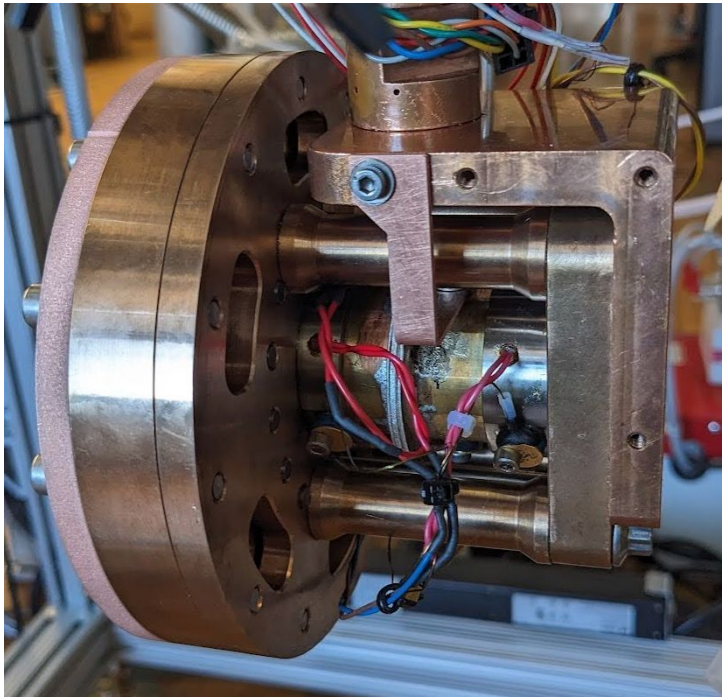

In-system compression of **liquid hydrogen** (2024)

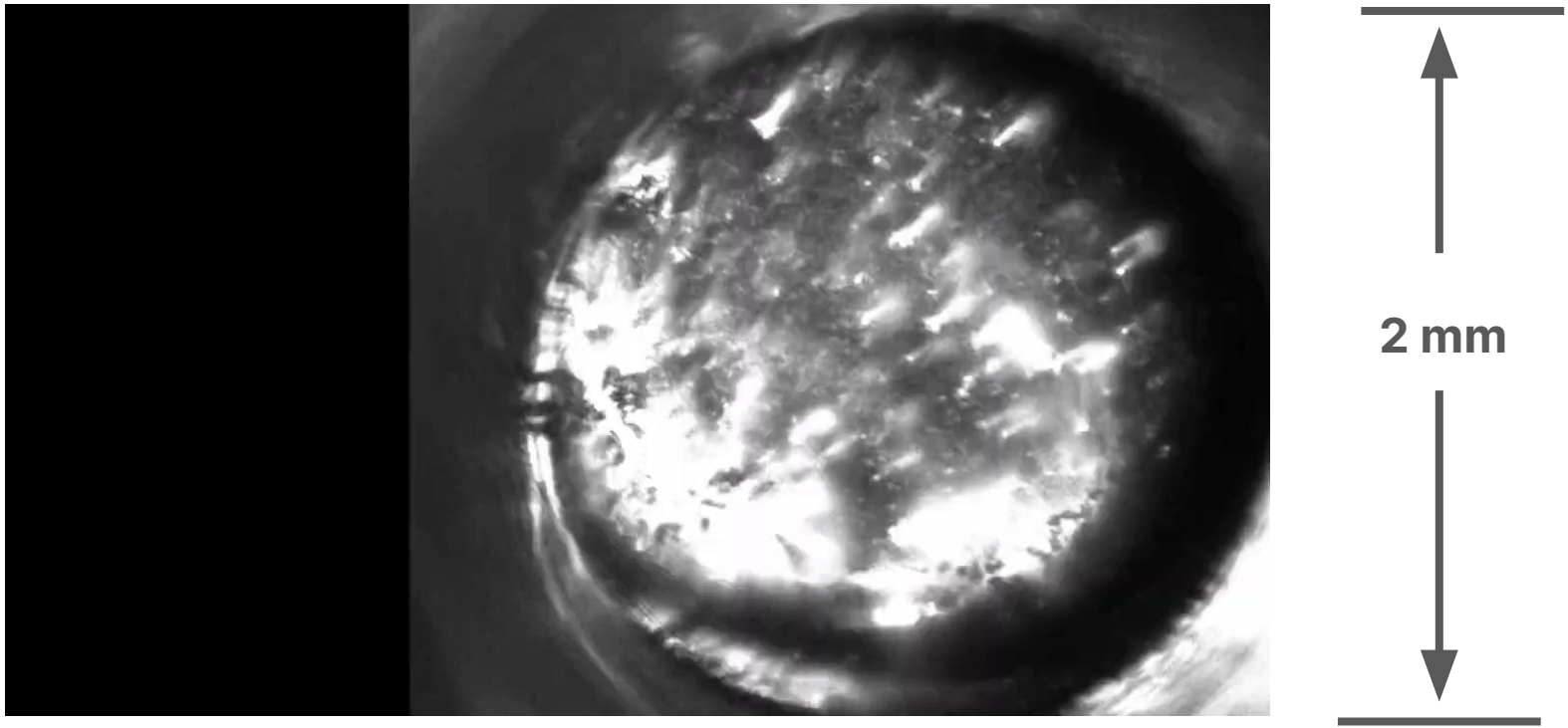

Filling the anvil cell with liquid hydrogen at 23 K. (Video at 16X speed)

In-system compression of **liquid hydrogen** (2024)

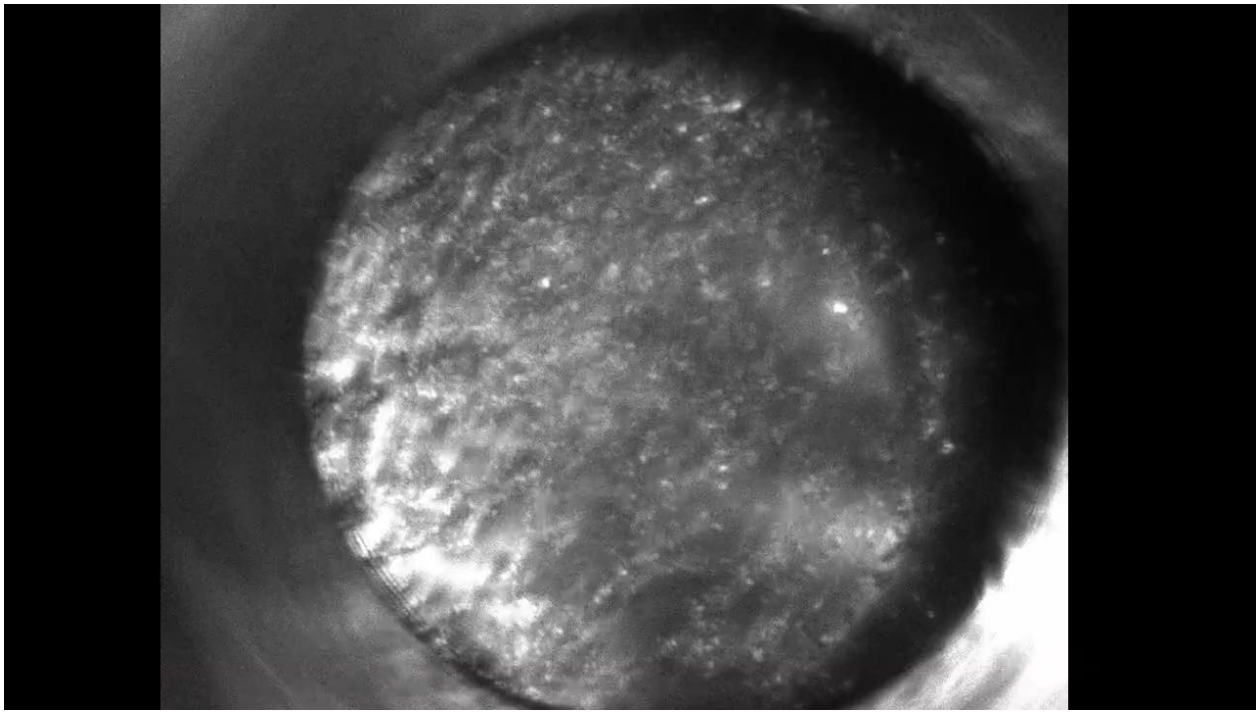

Video of the first compression step at t=8 min (Video at 1X speed)

Results

The hydrogen reached 650 MPa (94,000 PSI) (2024)

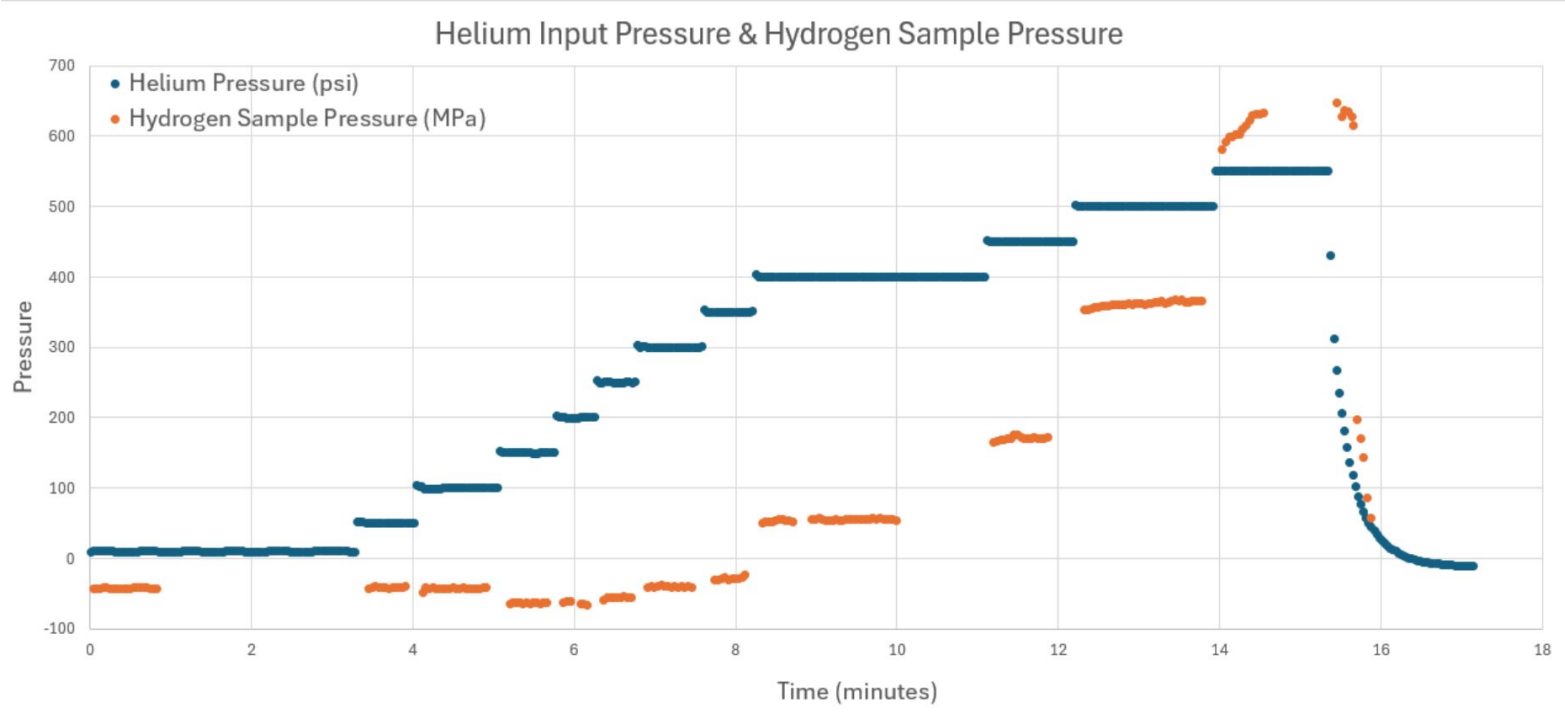

Map of beam time per cycling rate data point

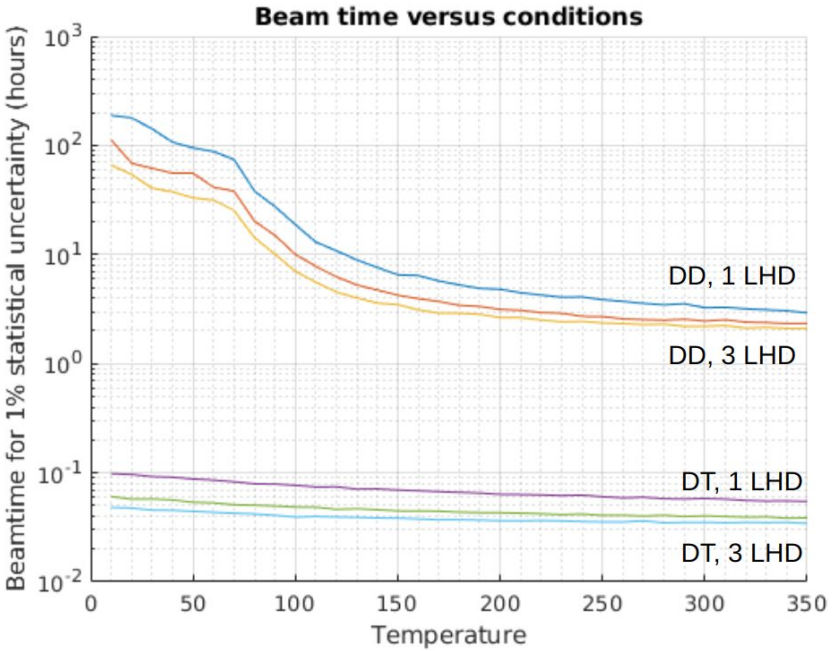

NOTE: From our simulations, measurement of the DT sticking fraction in the cell using the perpendicular neutron method requires 8 hours of beam.

Tritium gas handling system

- Walter Shmayda has joined our collaboration and is our tritium safety officer
- With PSI radiation safety, we have developed a safety plan, including hermetically sealed secondary containment and tritium scrubbers.
- Detail CAD design of the tritium gas handling system in underway

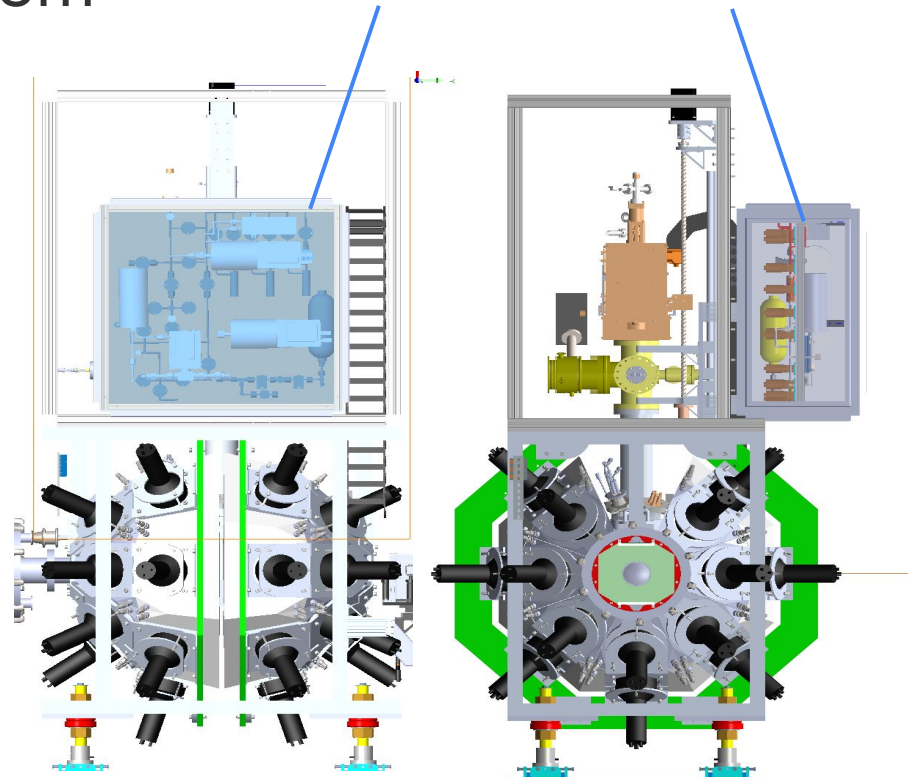

Planning

2024 Timeline and Beam Request

Tritium System Design

Tritium System Fabrication

Increase pressure and temperature range of anvil cell

Add perpendicular neutron and X-ray detectors

Measure and ensure gas purity

Setup At PSI (6 wks)

Beam (4 wks)

Data analysis

Summer vacations

Thanksgiving Nov 28

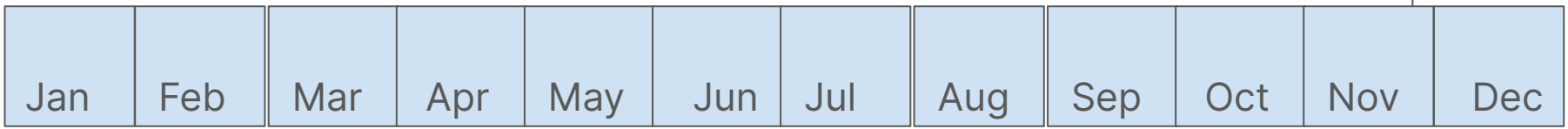

Acknowledgements

A. Adamczak[o], J.A. Allen[a], A. Antognini[c,m], E. G. Badaracco[d,i], J. Betances[a,n], N.J. Brennan[a], R. Chaney[a], W. Cutler[f,j], J. Davies[e], C. Forrest[e], A P. Gandhi[d], V. Glebov[e], A. Golossanov[c,f], D.M. Harrington[a], J.T. Hinchen[a], P.A. Holden[a], C. Izzo[d], C. Johnstone[d], J.D. Kalow[a], K. Kem[a], M. Khandaker[a], M. Kiburg[d], I. Kiniti[a,n], A.N. Knaian[a,c,d,f], L.E. Knaian[f], E. Koukina[f], K. Lau[a], J. Larson[k], K.R. Lynch[b,d], N.A. MacFadden[a,g], A. Mazzacane[d], P.A. McDaniel[a] , S.O. Newburg[a,f], E. Niner, K. Payne[a], C.C. Petitjean[c] , R. Ridgeway[d] , A. Sampat[a], W. Shamyda[e,l], W. Stadolnik[a,j], I.D. Spool[a] , S. Tripathy[b,d], D. Zajac[a,j]